Water-Soluble Reversible Coordination Polymers: Chains and Rings

Tina Vermonden,* Jasper van der Gucht, Pieter de Waard, Antonius T. M. Marcelis, Nicolaas A. M. Besseling, Ernst J. R. Sudhölter, Gerard J. Fleer, and Martien A. Cohen Stuart

Dutch Polymer Institute/Wageningen University, Laboratory of Organic Chemistry, Dreijenplein 8, 6703 HB Wageningen, Laboratory of Physical Chemistry and Colloid Science, Dreijenplein 6, 6703 HB Wageningen, and Wageningen NMR Centre, Dreijenlaan 3, 6703 HA, Wageningen, The Netherlands

Received June 24, 2003; Revised Manuscript Received July 16, 2003

ABSTRACT: The formation of soluble reversible coordination polymers with Zn^{2+} ions in aqueous solution was studied for two bifunctional ligands, differing in spacer length. Viscosity measurements were used to follow the formation of polymers as a function of the ratio between metal ions and ligands, the total ligand concentration, and the temperature. All the experimental findings could be reproduced and interpreted with a theoretical model that accounts for the formation of chains and rings. At low concentrations and at a 1:1 metal-to-ligand ratio, a large fraction of the ligand monomers are incorporated in small rings, with a small contribution to the viscosity. Rings are less important at higher concentrations or if one of the two components is in excess. The fraction of monomers in chains and rings could be estimated from ^{1}H NMR measurements, which were in good agreement with the model predictions. With increasing temperature, the fraction of monomers in rings decreases. As a result, the reduced viscosity increases with increasing temperature.

I. Introduction

In recent years there has been an enormous progress in the field of supramolecular chemistry.[1,2] One of the most interesting developments is the design of supramolecular equilibrium polymers. These are linear chains of small molecules held together by noncovalent, reversible interactions.[3−6] They reproduce many of the properties of traditional polymers but introduce also distinctly new features. For example, their molar mass distribution is not fixed but responds to variable conditions such as the monomer concentration, the temperature, and the presence of external fields, such as shear. An important class of supramolecular polymers is that of so-called coordination polymers.[7−15] In a coordination polymer the bonds between monomers are based on metal−ligand interactions. The associating molecules each have two ligand groups (L) that can form 1:2 complexes (ML_2) with metal ions (M). Addition of metal ions to a solution of these bifunctional monomers results in the formation of polymers, as depicted schematically in Scheme 1. There is an extensive literature about coordination polymers in the solid state, but the number of coordination polymers that has been characterized in solution is surprisingly small. Most soluble coordination polymers developed so far are based on kinetically stable metal−ligand interactions in noncoordinating solvents.[7−9] The exchange of ligands in such systems is extremely slow, so that the link between two monomers resembles a covalent bond. To design *reversible* coordination polymers, kinetically labile metal complexes must be used in coordinating solvents. Very few reversible coordination polymers have been studied so far.[10,11]

When a solution of bifunctional ligands is mixed with metal ions, two types of complexes can be formed as depicted in Scheme 1: linear chains and rings. In this paper a theoretical model for the coordination polymerization into rings and chains is developed in section II. In section III the experimental details are described, and in section IV we present the experimental results for two water-soluble bifunctional ligands with terdendate chelating groups. The bifunctional ligands are based on pyridine-2,6-dicarboxylic acid groups connected at the 4-position of the pyridine ring by tetra- or hexaethylene oxide spacers (Scheme 2). These chelating groups are known to form complexes with several transition metal ions such that one metal ion is coordinated by two terdendate ligand groups (6-coordination). Reversible polymers are formed when transition metal ions are added to a solution of these ligands. In this study we use Zn^{2+} as the metal ion because the

Scheme 1. Schematic Representation of the Formation of Polymers and Rings

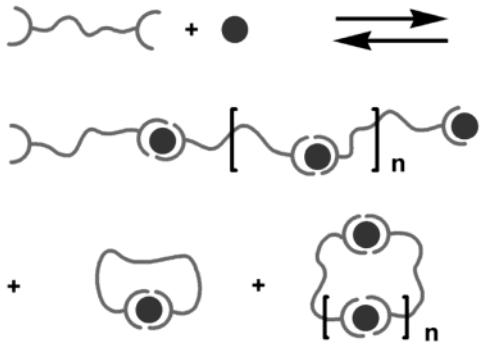

Scheme 2. Schematic Representation of Water-Soluble Bifunctional Ligands, C4 and C6

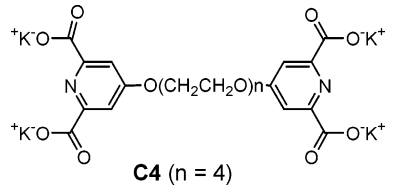

C4 (n = 4)
C6 (n = 6)

* Corresponding author: e-mail Tina.Vermonden@wur.nl.

10.1021/ma030353t CCC: $25.00
Published on Web 08/26/2003

coordination chemistry with the chelating groups is known and because its complexes are kinetically labile. Viscosity measurements are used to study the polymer formation as a function of the ratio between metal ion and ligand concentration, the total monomer concentration, and the temperature. An increase in viscosity indicates an increase in the average molar mass of the polymers. ^{1}H NMR measurements are used to estimate the fractions of monomers in chains and rings. The experimental results are compared to the theoretical predictions of the model described in section II.

II. Ring−Chain Equilibrium: Model Calculations

(a) Model. In this section, we present a method to calculate the molecular weight distributions of chains and rings based on the model of Jacobson and Stockmayer.[16] These authors considered the equilibrium between chains and rings in polycondensation polymers. Here, the model of Jacobson and Stockmayer is applied to solutions of coordination polymers. Coordination polymerization is analogous to polycondensations involving two different monomers that form an alternating copolymer (case III, "adipic acid−decamethylene glycol", in the paper of Jacobson and Stockmayer). In the present case, one type of monomer is the bifunctional ligand and the other is the metal ion.

Consider a solution of bifunctional ligands L_2 ("monomers") and metal ions M. Every monomer has two identical ligand groups L bridged by a spacer. The total molar concentration of monomers is C_{L_2}, and the total concentration of metal ions is C_M. We assume that the ligand groups can form two types of complexes with the metal ions: a 1:1 complex ML in which a metal ion is coordinated by one ligand group (and one or more solvent molecules) and a 1:2 complex ML_2 in which a metal ion is coordinated by two ligand groups. The ML_2 complexes are the bonds between two monomers, while the ML complexes or the free ligand groups L constitute the chain ends. We assume that all ligand groups react independently, i.e., the probability that a ligand group is involved in a certain type of complex does not depend on the degree of polymerization. The stability constants of the two types of complexes are defined as

$$K_1 = \frac{[ML]}{[M][L]} \tag{1}$$

$$K_2 = \frac{[ML_2]}{[ML][L]} \tag{2}$$

where [L], [M], [ML], and [ML_2] are the molar concentrations of free ligand groups, free metal ions, and metal ions coordinated by one and two ligand groups, respectively. For most coordination complexes, K_2 is smaller than K_1 because the first ligand group causes some repulsion for the second ligand group. This is different for alternating copolymers, for which the two stability constants are usually the same.

First, we consider the linear (open) chains. Let $c(n,m)$ be the concentration in moles per liter of chains of n monomers and m metal ions. Obviously, $|n - m| \leq 1$. Like for other equilibrium polymerizations, the distribution of chain lengths is exponential, as derived first by Flory[17]

$$c(n,m) = X_C C_{L_2} A_{n-m} (pq)^{n-1} \tag{3}$$

Here the factor p is the fraction of ligand groups in chains that are coordinated to a metal ion, and q is the fraction of these coordinated ligand groups that is involved in an ML_2 complex. Hence, the probability for a bond between two monomers (i.e., an ML_2 complex) is equal to pq, and the probability for $n - 1$ consecutive bonds is $(pq)^{n-1}$. The probabilities p and q are determined by the stability constants K_1 and K_2 and by the concentrations of monomers and metal ions. The factor X_C is a normalization constant, and A_{n-m} accounts for the probabilities of the chain ends. The probability for a ligand group in a chain to be free is $(1 - p)$, and the probability to form an ML complex is $p(1 - q)$. Hence

$$A_{n-m} = \begin{cases} (1-p)^2 & (n-m=1) \\ 2(1-p)p(1-q) & (n-m=0) \\ p^2(1-q)^2 & (n-m=-1) \end{cases}$$

The factor 2 for $n - m = 0$ takes into account that there are twice as many configurations for a chain with two different ends than for a chain with two identical ends. The total molar concentration of chains consisting of n monomers is

$$c(n) = c(n,n-1) + c(n,n) + c(n,n+1) = X_C C_{L2} (1-pq)^2 (pq)^{n-1} \tag{4}$$

and the total molar concentration of monomers incorporated in linear chains is found as $C_C = \sum_n nc(n) = X_C C_{L_2}$. Hence, the proportionality constant X_C in eq 3 gives the fraction of monomers in linear chains.

The equilibrium between rings and chains is determined by the difference in free energy between a chain and a ring of given length. When a chain is closed to form a ring, two end segments are removed (i.e., an ML complex and a free ligand group L react to form an ML_2 complex). This results in a negative free energy contribution. On the other hand, the conformational entropy is reduced upon ring closure, giving a positive free energy contribution. The equilibrium between rings and chains is a result of the balance between these two contributions. Jacobson and Stockmayer calculated the entropy difference between a chain and a ring, assuming that the chains and rings may be considered as ideal Gaussian chains. They derived the following distribution $r(n)$ for the rings:[16]

$$r(n) = B \frac{(pq)^n}{n^{5/2}} \quad (nv \geq 1) \tag{5}$$

with

$$B = \frac{10^{24}}{2N_{Av} l_k^3} \left(\frac{3}{2\pi v}\right)^{3/2}$$

where N_{Av} is Avogadro's number, l_k is the length of a statistical (Kuhn) segment expressed in nanometers, and v is the number of Kuhn segments per monomer. The Kuhn length[18] l_k is a measure for the stiffness of the monomers, and it depends on the type of spacer between the two ligand groups. The prefactor B has the dimension of concentration (moles per liter). From eq 5 we see that rings of many monomers are very unlikely. The reason for this is that the entropy loss upon ring closure is larger for long chains than for short ones. Moreover, rings are unimportant for very long spacers ($v \gg 1$) or for very stiff spacers (large l_k).

The Gaussian chain approximation is an adequate description for chains and rings of many Kuhn segments ($nv \gg 1$), but a serious oversimplification for small chains and rings. Shimada and Yamakawa used the wormlike chain model to predict ring-closure probabilities in the tight bending limit.[19] They showed that rings shorter than the Kuhn length ($nv < 1$) are strongly suppressed. Therefore, we explicitly forbid rings shorter than the Kuhn length here ($r(n) = 0$ for $nv < 1$), and we use eq 5 for $nv \geq 1$.

The total molar concentration of monomers in rings is

$$C_R = \sum_n nr(n) = B \sum_{n \geq v^{-1}} n^{-3/2}(pq)^n \quad (6)$$

and the fraction of monomers in rings is $X_R = 1 - X_C = C_R/C_{L_2}$.

The number-average length of the chains can be calculated as

$$\langle n_C \rangle = \frac{\sum_n nc(n)}{\sum_n c(n)} = \frac{1}{1 - pq} \quad (7)$$

For the chains the polydispersity index, defined as the weight-average length divided by the number-average length, equals $1 + pq$, which is approximately 2 if the average length is large ($pq \approx 1$). The number-average length of the rings is

$$\langle n_R \rangle = \frac{\sum_n nr(n)}{\sum_n r(n)} = \frac{\sum_{n \geq v^{-1}} n^{-3/2}(pq)^n}{\sum_{n \geq v^{-1}} n^{-5/2}(pq)^n} \quad (8)$$

and the total number-average length is

$$\langle n \rangle = \frac{\sum_n n[c(n) + r(n)]}{\sum_n [c(n) + r(n)]} \quad (9)$$

The length distributions of chains and rings are given in terms of the probabilities p and q. We will now relate these probabilities to the stability constants K_1 and K_2 and the concentrations of monomers and metal ions. The concentrations of the various species obey the mass conservation laws for monomers and metal ions:

$$2C_{L_2} = \alpha[L] + [ML] + 2[ML_2] \quad (10)$$

$$C_M = [M] + [ML] + [ML_2] \quad (11)$$

The factor 2 on the left-hand side of eq 10 is added because each monomer has two ligand groups. The factor α accounts for the protonation of the ligand groups:

$$\alpha = 1 + [HL]/[L] + [H_2L]/[L] + \ldots = 1 + K_{a1}[H] + K_{a2}[H]^2 + \ldots \quad (12)$$

where H denotes a proton, and $K_{a1} = [HL]/[H][L]$ and $K_{a2} = [H_2L]/[H]^2[L]$ are the first and second protonation constant, respectively. At high enough pH the protonation of the ligands may be neglected.

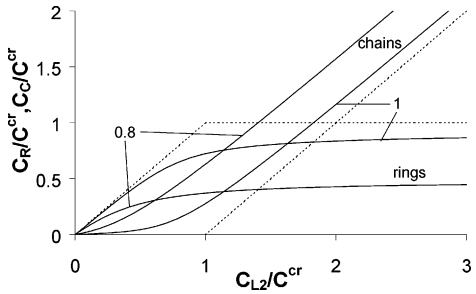

Figure 1. Theoretical: concentrations of monomers in rings (C_R) and chains (C_C) (normalized with respect to C^{cr}) as a function of monomer concentration for metal-to-monomer ratios of 1 and 0.8 (as indicated), with $l_k = 3$ nm, $v = 3$, $K_1 = 10^7$, and $K_2 = 10^6$. The dashed lines correspond to infinite values of K_1 and K_2 at a 1:1 ratio.

The concentrations of free ligand [L], and of the two types of complexes [ML] and [ML_2], can be found from the chain and ring distributions $c(n,m)$ and $r(n)$ by counting the number of end segments and bonds:

$$\alpha[L] = \sum_n [2c(n,n-1) + c(n,n)] = 2X_C C_{L2}(1 - p) \quad (13)$$

$$[ML] = \sum_n [c(n,n) + 2c(n,n+1)] = 2X_C C_{L2} p(1 - q) \quad (14)$$

$$[ML_2] = \sum_n [(n-1)c(n) + nr(n)] = X_C C_{L_2} pq + B \sum_{n > v^{-1}} n^{-3/2}(pq)^n \quad (15)$$

Substitution of eqs 13−15 in eqs 1, 2, 10, and 11 gives four equations that can be solved numerically to find p, q, X_C, and [M] for given values of the stability constants and monomer and metal concentrations.

(b) General Trends. In this section we present some general trends for the equilibrium between chains and rings as predicted by the model. In section IV, we compare the model to the experimental data, using specific values of the various parameters.

The total concentration of monomers in rings is given by eq 6. From this equation, we can see that for a given type of monomers (i.e., given v and l_k), there is an upper limit C^{cr} to the concentration of monomers in rings. The maximum value that the probabilities p and q can have is unity (for high stability constants, at high monomer concentration and at a 1:1 metal-to-ligand ratio), so that

$$C^{cr} = B \sum_{n \geq v^{-1}} n^{-3/2} \quad (16)$$

For $v \geq 1$, this gives $C^{cr} \approx 2.6B$.

The concentrations of monomers in chains and rings as a function of the total concentration are shown in Figure 1 for two metal/monomer ratios y and with $l_k = 3$ nm, $v = 3$, $K_1 = 10^7$, and $K_2 = 10^6$. We examine the case that pH $\gg$ pK_{a1}, pK_{a2}, so that the protonation is negligible. The concentrations have been divided by C^{cr} (which is 5.1 mM for the parameters used). Clearly, at low concentrations most monomers are incorporated in rings, while at higher concentrations chains become

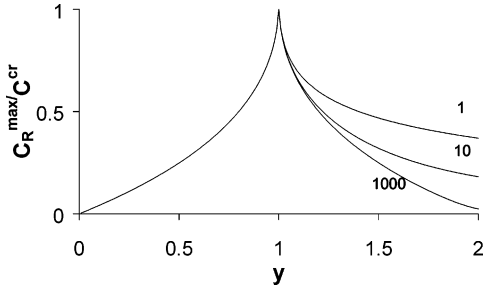

Figure 2. Theoretical: plateau of the concentration of monomers in rings (normalized with respect to B) as a function of the metal/monomer ratio y for various ratios K_1/K_2.

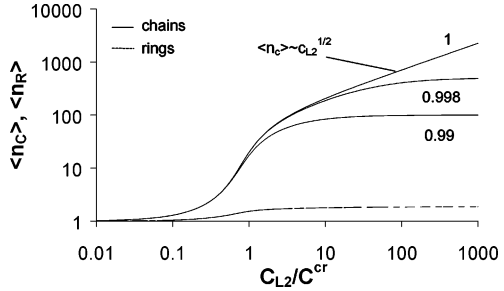

Figure 3. Theoretical: number-average length of chains and rings as a function of the monomer concentration for several metal/monomer ratios. Same parameters as in Figure 1.

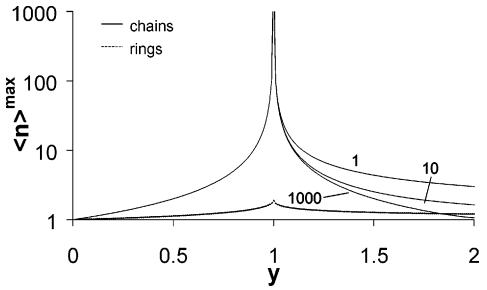

Figure 4. Theoretical: maximum values of the average length of chains and rings as a function of the metal/monomer ratio y for several ratios K_1/K_2.

more important. For $y \equiv C_M/C_{L2}$ equal to unity and low concentrations, $C_R \approx C_{L_2}$, while at higher concentrations ($C_{L_2} \gg C^{cr}$) the concentration of rings goes asymptotically to a plateau, given by $C_R \approx C^{cr}$. Hence, $2C^{cr}$ can be regarded as the concentration below which rings dominate and above which chains dominate (for $y = 1$). For finite values of the stability constants the transition from the ring-dominated regime to the chain-dominated regime is rather smooth, but it becomes sharper if the stability constants become larger. For infinite values of K_1 and K_2 at $y = 1$ (the dashed lines in Figure 1), C^{cr} may be considered as a critical concentration at which the formation of chains starts. (This is analogous to the critical micelle concentration in surfactant systems.) This can also be seen from eqs 13−15: for infinite K_1 and K_2, and $C_M = C_{L_2}$, both [L] and [ML] are equal to zero, while $[ML_2] = C_{L_2}$. According to eqs 13 and 14, this means that either $X_C = 0$ or p and q are equal to unity. From eqs 15 and 16, we see that p and q must be smaller than unity if $C_{L_2} < C^{cr}$, while X_C must be larger than zero for $C_{L_2} > C^{cr}$. Hence, we have $C_C = 0$ and $C_R = C_{L_2}$ for concentrations below C^{cr}, whereas $C_R = C^{cr}$ and $C_C = C_{L_2} - C^{cr}$ for concentrations above C^{cr}.

If the ratio y between monomers and metal ions is not equal to unity, rings are less prominent because the excess component can form extra chain ends. The maximum concentration of rings for this case is smaller than C^{cr}. In Figure 2, we have plotted the plateau value of the ring concentration C_R^{max} as a function of y for several values of the stability constants. For an excess of monomers ($y < 1$), the maximum ring concentration is determined by y only. The probability p that a monomer in a chain is coordinated to a metal ion is at most $y = C_M/C_{L_2}$ for this case, while q is close to unity at high concentrations. For example, for $y = 0.8$ (shown in Figure 1), the maximum value of p is 0.8, and we find from eq 6 that the maximum concentration of monomers in rings is equal to $1.2B \approx 0.46C^{cr}$. As we can see in Figure 2, for an excess of metal ions ($y > 1$), the maximum ring concentration depends on the ratio between the stability constants. The probability p is close to unity for this case, while q is determined by the ratio K_1/K_2. Rings are favored if ML_2 complexes are relatively stable, which is the case if K_2 is large compared to K_1.

The number-averaged length of the chains and the rings is plotted in Figure 3 as a function of the monomer concentration for several values of y and the same parameters as in Figure 1. As expected, the chains are much larger than the rings. With increasing concentration, both chains and rings become larger. The average size of the rings remains small and goes to a plateau value at high monomer concentrations. From eq 7 we can find the maximum value of the average size of the rings by setting p and q equal to unity. For monomers with $v \geq 1$ the maximum average ring size is 1.9 monomers (at a 1:1 ratio). For other ratios, the average size is slightly smaller. The chains, on the other hand, become much longer. For $y = 1$, the average length of the chains at high concentrations increases with C_{L_2} as

$$\langle n_c \rangle = \sqrt{K_2 C_{L_2}} \quad (C_M = C_{L_2} \gg C^{cr}) \tag{17}$$

This is similar to other equilibrium polymers.[20] It can be found from eqs 2, 10, and 11, by taking $C_{L_2} \approx [ML_2] \gg [ML] \gg [M]$ and using $\langle n_c \rangle = 2C_{L_2}/([L] + [ML])$ (which is valid if rings can be neglected, i.e., for $C_{L_2} \gg C^{cr}$). For $y \neq 1$ the average length is smaller and goes to a plateau at high concentrations. Figure 4 shows the plateau of the average length of the chains and the rings as a function of y for several ratios K_1/K_2. Obviously, for $y = 1$, the average length of the chains does not reach a plateau but increases with concentration according to eq 17. For $y < 1$, the average chain length depends only on the value of y. Since p can reach a maximum value of $y = C_M/C_{L_2}$ and q is close to unity, the maximum of the average length is, according to eq 7,

$$\langle n_c \rangle^{max} = \frac{C_{L_2}}{C_{L_2} - C_M} \quad (C_M < C_{L_2}) \tag{18}$$

For $y > 1$, the average chain length depends on the ratio between the two stability constants, just like the maximum ring concentration in Figure 2. The average length is larger if ML_2 complexes are favored; i.e., if K_2 is large compared to K_1. For a small excess of metal, the curve in Figure 4 is symmetric around the peak, and the average length $\langle n_c \rangle^{max}$ is given by $C_M/(C_M - C_{L_2})$. It can be seen in Figure 4 that the rings also have a maximum length for $y = 1$, but even at the peak it is still very small.

In this section we presented some general results for coordination polymerization into chains and rings. We investigated the effect of the metal/monomer ratio and the total monomer concentration on the equilibrium between chains and rings and their average lengths. In section IV, we will compare the model to experimental data for two water-soluble bifunctional terdentate ligands.

III. Experimental Section

All commercial chemicals were obtained from Acros or Aldrich and were used as received. Chelidamic acid was purchased from Acros. Diethyl 4-hydroxypyridine-2,6-dicarboxylate[21] and dibromooligoethylene oxide[22] (tetra and hexa) were prepared according to the literature. ^{1}H NMR (200 MHz) and ^{13}C NMR spectra were recorded on a Bruker AC-E 200 spectrometer. DOSY−NMR (400 MHz) spectra were recorded and calculated using standard Bruker software on a Bruker DPX 400 spectrometer at room temperature. Isothermal titration calorimetry measurements are performed on a Microcal MCS ITC. Viscosity measurements were performed in a 100 mM 1,4-piperazinebis(ethanesulfonic acid) buffer (PIPES), pH 5.4, on a LAUDA processor viscosity system PVS1. The reduced viscosity is defined as the specific viscosity divided by the ligand concentration C in grams per liter, $\eta_{red} = \eta_{sp}/C = (\eta_s - \eta_0)/(\eta_0 C)$ with η_s the viscosity of the sample and η_0 the viscosity of the solvent.

Synthesis of 1,11-Bis(2,6-dicarboxypyridin-4yloxy)-3,6,9-trioxaundecane, C4, and 1,17-Bis(2,6-dicarboxypyridin-4yloxy)-3,6,9,12,15-pentaoxaheptadecane, C6. Diethyl 4-hydroxypyridine-2,6-dicarboxylate (2.99 g, 12.5 mmol), 6.25 mmol of dibromooligoethylene oxide (tetra or hexa), and 4.2 g of K_2CO_3 were refluxed in 2-butanone for 3 days under a N_2 atmosphere. The reaction can be followed by TLC analysis using 5% MeOH in CH_2Cl_2 as eluents. The solvent was removed, and a 1:1 mixture of ethanol−water was added. This mixture was stirred overnight at 70 °C. The resulting water-soluble product was purified by C_{18} reversed-phase chromatography (40 μm prep. LC) using water as eluent. This purification step was repeated several times. After this treatment compound **C6** was pure. Compound **C4** was purified further using size exclusion chromatography (Sephadex G10, water as eluent). The products were freeze-dried.

C4: yield 20% (mp > 300 °C). ^{1}H NMR (D_2O): δ 3.50 (8H, m, CH_2O), 3.71 (4H, t, CH_2O), 4.14 (4H, t, CH_2O), 7.33 (4H, s, aromatic H). ^{13}C NMR (D_2O): δ 69.68, 70.73, 71.65, 71.84, 113.64, 156.18, 169.28, 173.83.

C6: yield 18% (mp > 300 °C). ^{1}H NMR (D_2O): δ 3.46 (16H, m, CH_2O), 3.71 (4H, t, CH_2O), 4.14 (4H, t, CH_2O), 7.34 (4H, s, aromatic H). ^{13}C NMR (D_2O): δ 69.88, 71.05, 71.97, 72.09, 72.10, 72.12, 113.88, 156.90, 169.26, 173.81.

IV. Experimental Results and Discussion

Water-soluble bifunctional ligands **C4** and **C6** (see Scheme 2), with four and six ethylene oxide units as spacer, were synthesized in three steps from commercially available chelidamic acid. The acid groups were first protected as ethyl esters,[21] after which the appropriate dibromooligoethylene oxide spacer[22] was coupled to the aromatic OH group using K_2CO_3 as a base. In the last step the ester groups were hydrolyzed, yielding the final ligands **C4** and **C6** as potassium salts.

These ligands and their complexes with Zn^{2+} are water-soluble over a wide pH range. The complexation gives an almost undetectable change in the UV spectra of the ligands upon addition of a Zn^{2+} solution, but the stoichiometry of complexation was confirmed by isothermal titration calorimetry (ITC) measurements. Besides stoichiometry, ITC measurements also give information about the complexation constants. However, when the constants are very high ($K > 10^5$ M^{-1}), it is difficult to obtain these values accurately with this method. On the basis of the ITC measurements, we conclude that the complexation constants between the ligands and Zn^{2+} ions are larger than 10^5 M^{-1}. Complexation constants reported by Anderegg[23] of structurally equivalent 2,6-pyridinedicarboxylic acid and Zn^{2+} ions confirm our results: $K_1 = 10^{6.4}$ and $K_2 = 10^{5.5}$ for the 1:1 and 1:2 complexes, respectively. Anderegg reported also acidity constants for the same ligands: $K_{a1} = 10^{4.7}$ and $K_{a2} = 10^{6.8}$. Proton titrations with our ligands suggest that K_{a1} and K_{a2} are somewhat larger than this. We tried measuring the stability constants K_1 and K_2 using proton titrations in the presence of Zn^{2+}, but unfortunately we did not succeed because the stability constants are too high to measure with this method. The measurements do suggest, however, that K_1 and K_2 for our ligands are also somewhat higher than reported by Anderegg. Model calculations indicate that the behavior is rather insensitive to the values of the stability constants. In fact, the model results are hardly affected if all K values are made larger by a factor of 100. Therefore, in our calculations we use the values reported by Anderegg for K_1, K_2, K_{a1}, and K_{a2}. The value of α with these values is 1.2 at pH 5.4.

To compare the experimental results described in this section to model calculations, we need realistic values for l_k and ν. A molecular model shows that for the ligand with the shortest spacer **C4** at least two monomers are needed for a ring, while the one with the longest spacer **C6** is just able to form an intramolecular complex (a ring of one monomer) without strain in the ring. Hence, we take the Kuhn length equal to the length of the largest molecule: $l_k = 3.3$ nm. We furthermore assume that the Kuhn length is the same for the two monomers. This is an oversimplification because the relative contribution of the stiff complexed chelidamic acid groups is larger for **C4** than for **C6**, but here we neglect this. The length of **C6** is about 3.3 nm (i.e., $\nu = 1$), and that of **C4** is about 2.7 nm (i.e., $\nu = 0.83$). With these parameters we find that the maximum concentration of monomers in rings C^{cr} is 19.8 mM for $\nu = 1$ (**C6**) and 16.2 mM for $\nu = 0.83$ (**C4**). We note that the estimation of the various parameters in the model is somewhat crude, but the choice of the parameters does not change the results qualitatively.

(a) Molar Ratio Dependence. We measured the reduced viscosity as a function of the molar ratio Zn^{2+}:bifunctional ligand for both ligands in buffer. The pH (=5.4) was chosen high enough to favor metal complexation over protonation of the ligands and low enough to prevent the formation of insoluble zinc hydroxide. Figure 5a displays the reduced viscosity of ligand **C4** as a function of the molar ratio Zn^{2+}:**C4** for two concentrations of **C4**. In the experiments a concentrated $Zn(ClO_4)_2$ solution (approximately 1.0 M) was titrated to the ligand solution. After mixing, the viscosity reached equilibrium immediately. It is well-known that the reduced viscosity of polymer solutions increases with the average chain length of the polymers. We observe an increase in reduced viscosity for increasing molar ratio until a ratio of 1 is reached. Beyond a ratio of 1, it decreases again. Excess of either bifunctional ligands or metal ions will yield extra chain ends. Since for linear chains the average number of monomers per chain is inversely proportional to the number of chain ends, the viscosity decreases again at molar ratios larger than 1. That this decrease occurs implies that the complexes

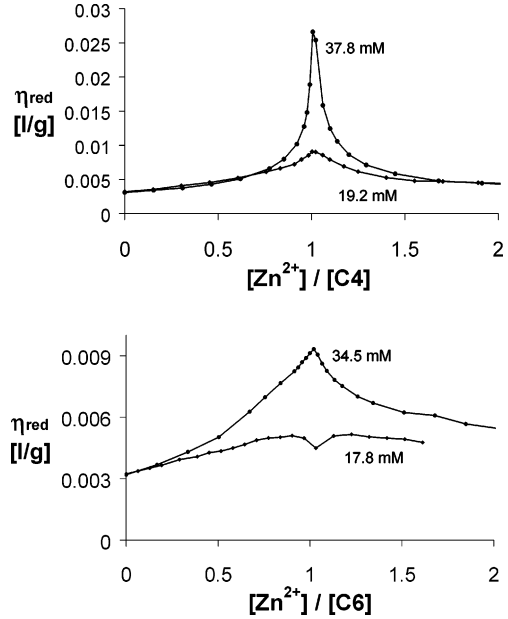

Figure 5. Experimental: reduced viscosity of ligands as a function of molar ratio $Zn(ClO_4)_2$/ligand in 0.1 M PIPES buffer pH 5.4 at 298 K for (a) ligand **C4** (12.7 and 25.6 g/L) and (b) ligand **C6** (13.4 and 26.9 g/L).

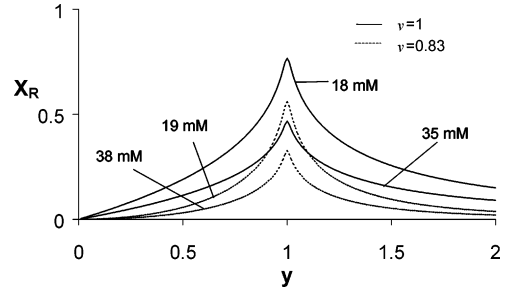

Figure 6. Theoretical: weight fraction of monomers in rings X_R as a function of the metal/monomer ratio y and monomer concentration for monomers with $v = 0.83$ and $v = 1$ at the concentrations used in the experiments.

are reversible, so that the chains that are formed initially break up. For a ligand concentration approximately twice as high, a 3 times higher reduced viscosity was found. This indicates that longer polymers are formed at higher concentrations.

For ligand **C6**, with a longer spacer a radically different plot is observed (Figure 5b). For the highest concentration of 34.5 mM a peak was found at a molar ratio of 1. The shape of the curve is the same as for **C4**. However, the peak is not as high as for a similar concentration of **C4**. Surprisingly, for the lower concentration of 17.8 mM a dip in the curve was found at a molar ratio 1, instead of a peak. At first we were rather puzzled by this, but it turns out that the model described in section II can explain these results in terms of ring formation.

Figure 6 shows the theoretical weight fractions of monomers in rings X_R as a function of the ratio between the metal and monomer concentration y for both monomers at the concentrations used in the experiments. As already explained in section II, rings are most important at low concentrations and at a 1:1 metal:ligand ratio. We see in Figure 6 that the fraction of rings is slightly lower for the monomers with a shorter spacer ($v = 0.83$) than for the monomers with the longer spacer ($v = 1$). The reason for this is that the shorter monomer needs

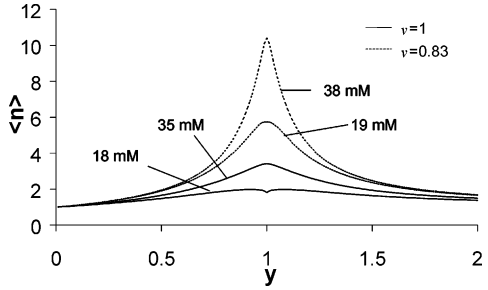

Figure 7. Theoretical: total average length as a function of y for $v = 0.83$ and $v = 1$ (corresponding to **C6** and **C4**) matching the experimentally used concentrations.

at least two monomers to form a ring. As a result, C^{cr} is somewhat smaller for $v = 0.83$ (**C4**) than for $v = 1$ (**C6**).

Because rings have a smaller degree of polymerization and a more compact conformation than linear chains (see Figures 3 and 4), the viscosity is lower in the region where rings are most abundant. In Figure 7 we have plotted the calculated total average length $\langle n \rangle$ as a function of y for the two monomers and for the concentrations used in the experiments. It can be seen that for the monomers with $v = 1$ the average length $\langle n \rangle$ has a dip at the lowest concentration at $y = 1$, as has the viscosity of **C6**. At this ratio almost all monomers are in rings as can be seen in Figure 6. Because the rings are very small, the viscosity has a minimum at $y = 1$. At higher concentrations ($C_{L_2} \gg C^{cr}$) the dip vanishes because rings are less important then. For the monomers with the shorter spacer ($v = 0.83$) the dip does not occur, just like in the viscosity measurements. At least two monomers are needed for a ring in this case, and as a result the amount of rings is smaller.

(b) Concentration Dependence. In section II, we have seen that the fraction of monomers in rings is a function of the total concentration of monomers. Experimentally, the concentrations of monomers in chains and rings can be measured with ^{1}H NMR spectroscopy provided rings and chains give rise to different peaks in the spectrum. Indeed, two sets of signals are obtained in the ^{1}H NMR spectra of monomer and metal ion at a 1:1 ratio. To assign the peaks correctly to the different species DOSY NMR (diffusion ordered spectroscopy),[24] experiments were performed. Figure 8 shows the DOSY spectrum for **C4** and Zn^{2+} ions in a 1:1 ratio at 36 mM in D_2O. On the horizontal axis the proton NMR spectrum is plotted, and on the vertical axis the logarithm of the diffusion coefficient (D) corresponding to the proton peaks is plotted. The peaks on the horizontal axis (^{1}H NMR spectrum) between 3.5 and 4.7 ppm originate from the OCH_2 groups in the spacer. The singlets around 7.8 ppm originate from the aromatic protons of the pyridine ring. The residual solvent peak is very large and therefore gives a high DOSY signal. The solvent signal has the highest intensity at $\log D = -8.62$, which corresponds to the diffusion coefficient of water at 25 °C of 2.4×10^{-9} m^2/s. Two groups of peaks can be seen in the DOSY spectrum. One group (denoted with an R) has a maximum intensity at $\log D = -8.9$ (or $D = 1.2 \times 10^{-9}$ m^2/s). The other (denoted with a C) give signals over a wide range of diffusion coefficients from about $\log D = -9.5$ ($D = 3.1 \times 10^{-10}$ m^2/s) to the measurement limit of $\log D = -10.1$ ($D = 7.9 \times 10^{-11}$ m^2/s). It may be expected that the rings are smaller than the chains (see Figures 3 and 4), so that they have a larger diffusion coefficient. Hence, we assume that the peaks with a high

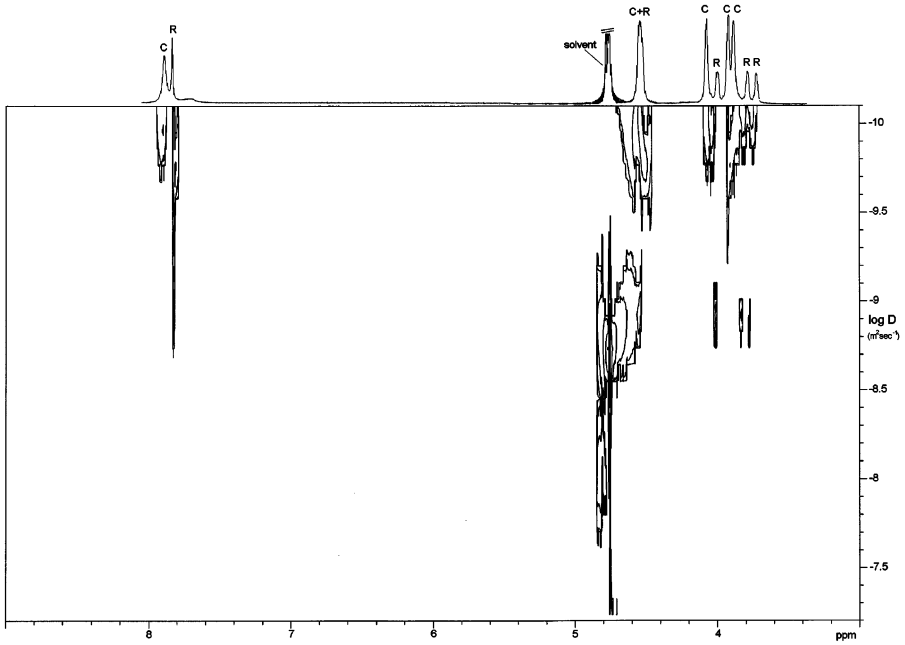

Figure 8. DOSY-NMR spectrum of a 36 mM of **C4** and Zn^{2+} solution in D_2O at 298 K. The signal of HDO is cut off.

diffusion coefficient (denoted with an R) correspond to rings, while those with a lower diffusion coefficient (denoted with a C) correspond to chains. Larger compounds give broader peaks in ^1H NMR spectra, which is another indication that the broad peaks correspond to protons in chains and the sharp peaks to the smaller cycles. For the triplet signals of the OCH_2 groups it is hard to see the difference in sharpness of the peaks for chains and rings, but for the singlet signal at about 7.8 ppm the peak of the chains is much broader than of the rings. For one of the peaks (4.4−4.5 ppm) the ring and chain signal overlap. The large range of diffusion coefficients for the chains can be explained by their polydispersity. An exponential chain length distribution is expected (see eqs 3 and 4). Most peaks denoted with an R also show some signals in the same region of diffusion coefficients as the peaks denoted with a C. The explanation for the different diffusion coefficients belonging to one peak is that molecules exchange between cyclic and open structures on the time scale of the measurement. This exchange was also proven by a ROESY-NMR (rotating frame nuclear Overhauser enhancement spectroscopy) experiment, which showed cross-peaks due to through bond coupling between R and C signals. The time scale of both 2D experiments (DOSY and ROESY) is about 200 ms, which is much larger than for the 1D proton spectra. The exchange between rings and chains on the time scale of the 1D proton spectra can be neglected.

Figure 9 shows the ^1H NMR spectra for compound **C4** and Zn^{2+} ions at a 1:1 ratio in D_2O at 298 K at different concentrations. The spectrum at the lowest concentration (Figure 9c) resembles the spectrum of the ligand molecules without metal ions present. However, the chemical shifts are different, which indicates that the metal ions are bound to the ligand, as already expected from the known association constants. The most notable difference is the number of peaks originating from the spacer. Without metal ions present the spacer shows only three signals instead of four because two of them have the same chemical shift, which is not the case when metal ions are present.

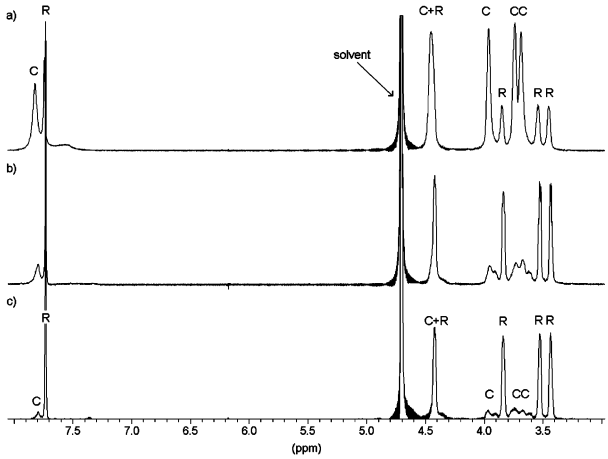

Figure 9. ^1H NMR spectra of compound **C4** with Zn^{2+} (1:1 ratio) in D_2O at 298 K at various concentrations: 36 (a), 13 (b), and 6.5 mM (c). Signals assigned to chains and rings are denoted with C and R, respectively.

The spectra at different concentrations show the two sets of signals denoted with C (chains) and R (rings) that are assigned on the basis of the DOSY-NMR results and the sharpness of the peaks. At low concentrations the ring signals are very high compared to the chain signals. Upon increasing the concentration the chain signals become larger.

^1H NMR spectra for compound **C6** and Zn^{2+} at a 1:1 ratio also gave two sets of signals that could be ascribed to rings and chains (not shown). As expected, the peaks ascribed to chains increase with concentration, but they are lower than for the **C4** system at the same concentrations. The relative amounts of rings and chains can be determined from the integrals of the peaks in the 1D proton spectra, since exchange between rings and chains can be neglected here. Figure 10 shows the concentrations of both monomers, **C4** and **C6**, in chains and rings as a function of the total monomer concentration. Clearly, at low concentrations most monomers are incorporated in rings, while at higher concentrations chains are more important. At higher concentrations,

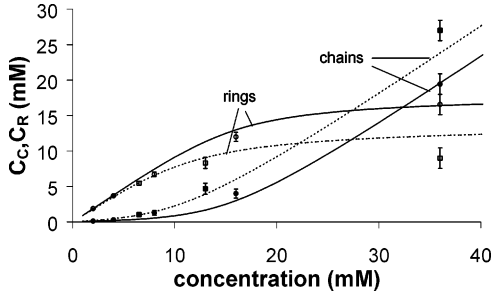

Figure 10. Concentrations of monomers in chains (**C4**, ■; **C6**, ●) and rings (**C4**, □; **C6**, ○) as a function of the monomer concentration with Zn^{2+} (1:1 ratio) in D_2O at 298 K, determined from the integrals of the peaks in ^1H NMR spectra. The curves refer to results of the theoretical model: full curves $\nu = 1$ and $l_k = 3.3$ nm (corresponding to **C6**); dashed curves $\nu = 0.83$ and $l_k = 3.3$ nm (corresponding to **C4**).

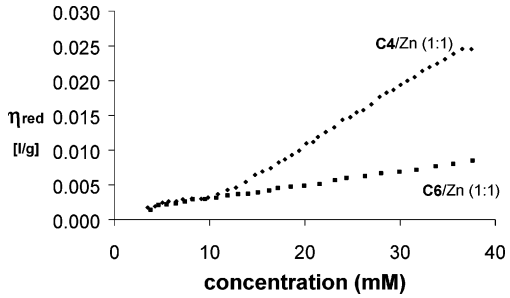

Figure 11. Reduced viscosity of ligands **C4** and **C6** as a function of concentration at a $Zn(ClO_4)_2$/ligand ratio of 1 in 0.1 M PIPES buffer pH 5.4 at 298 K.

the concentration of monomers in rings seems to level off toward a constant value, as predicted by the model (Figure 1). For **C4** the concentration of rings is lower than for **C6** at the same overall concentration. This is caused by the possibility of **C6** to form monomeric rings, while **C4** needs at least two monomers for a ring. In the same figure the results of the model calculations are shown for both monomers (the full and dashed curves). The agreement between the experimental data and the theoretical curves is very good, especially for **C6** ($\nu = 1$). For **C4** ($\nu = 0.83$) the agreement is not as good as for **C6**. The model overestimates the amount of rings. The reason for this may be that we have used the same value for the Kuhn length for both **C4** and **C6**. In reality, however, the Kuhn length is probably somewhat higher for **C4** than for **C6** because the stiff ligand groups are relatively more important for the smaller monomer. We note that, by choosing a larger value for the Kuhn length (4 nm), we can obtain a very good agreement between experiment and theory for the **C4** monomers, too.

In Figure 5 we have seen that the reduced viscosity depends on the concentration of monomers. With increasing concentration the fraction of monomers in rings decreases, as seen from the NMR measurements. Also, the average length of the chains and rings increases with increasing concentration (see Figure 3). Figure 11 shows the reduced viscosity of compounds **C4** and **C6** as a function of the concentration at a metal−ligand ratio close to 1 (within 0.5%), at pH 5.4 and 298 K. For low concentrations the increase in viscosity with increasing concentration is small. At these concentrations mainly small rings are present, with only a small influence on the viscosity. For **C4** the viscosity starts to increase more steeply at a concentration of about 11−13 mM. This is caused by the formation of more (and

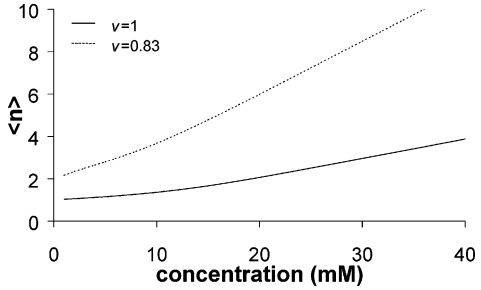

Figure 12. Theoretical: total average length as a function of the monomer concentration for a metal/monomer ratio equal to unity for $\nu = 0.83$ and $\nu = 1$.

larger) linear chains at these concentrations (see Figure 10). For **C6** the effect of the concentration is somewhat different. The slope of the first part of the curve is the same as for **C4,** but the increase in viscosity above 11−13 mM is much smaller. This is probably caused by the larger amount of rings (mainly monomers) present at all concentrations in the solution of **C6** (see Figure 10).

As already explained, the viscosity of a polymer solution is determined by the average size of the molecules. In Figure 12, we have plotted the concentration dependence of the total average length $\langle n \rangle$, calculated using the model of section II for both ligands at a metal/monomer ratio equal to unity. The increase in chain length with concentration is obvious. At low concentrations, all monomers are in rings, and the average length is equal to the size of a minimal ring: one for **C6** and two for **C4**. With increasing concentration, the average size increases, mainly because the rings become larger. Above a certain concentration ($\approx C^{cr}$), the increase of the average length becomes more steep because chains start to grow. For $\nu = 0.83$ the increase in average length is faster than for $\nu = 1$. The shape of the calculated curves is in qualitative agreement with the viscosity data in Figure 11. For **C4** a change of slope is observed at a concentration of around 12 mM, which can also be seen in the calculated curve of Figure 12. For **C6** the viscosity increases more slowly with concentration, just like the calculated average length. We note that the increase of the viscosity with concentration is caused not only by an increase of the average length but also by the difference in conformation of chains and rings. Because the structure of a ring is more compact than that of a chain, its contribution to the viscosity is probably smaller than that of a chain of the same size.

(c) Temperature Dependence. ^1H NMR spectra of 6.5 mM of **C4** and Zn^{2+} (1:1) in D_2O at different temperatures reveal a strong temperature dependence of the ring−chain equilibrium (see Figure 13). With increasing temperature the ring peaks become smaller and the chain peaks become larger. Upon cooling, the initial spectra were found again, which confirms the reversibility of the system. At higher temperatures there is some overlap between ring and chain peaks, and when the temperature exceeds 333 K, the different peaks are hardly discernible. Because of this overlap, the values of the integrals of both types of peaks become less accurate for increasing temperature. Furthermore, the solvent peak shifts to lower ppm values (from 4.8 to 4.4) due to increasing temperature. It overlaps with one of the sample peaks at these temperatures, which makes it difficult to interpret that part of the spectrum. Nevertheless, we estimated the fraction of monomers

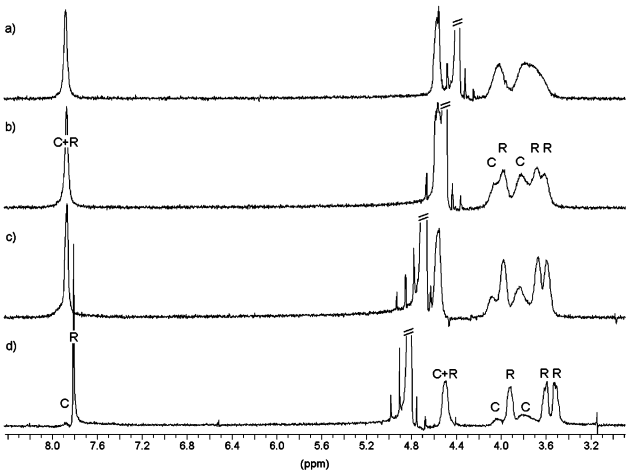

Figure 13. ^{1}H NMR spectra of a 6.5 mM solution of **C4** and Zn^{2+} (1:1 ratio) in D_2O at various temperatures: 343 (a), 333 (b), 318 (c), 303 K (d). Signals from chains and rings are denoted with C and R, respectively. The signal of HDO is cut off.

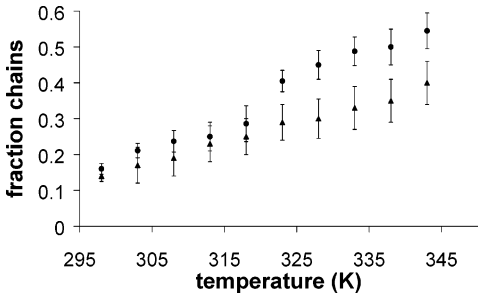

Figure 14. Fraction of chains of ligands **C4**, 6.5 mM (●), and **C6**, 8.0 mM (▲), as a function of temperature in D_2O at a $Zn(ClO_4)_2$/ligand ratio of 1, determined from the integrals of the peaks in ^{1}H NMR spectra.

in chains and rings from the integrals of the peaks. The results are plotted in Figure 14. Although the error bars are large due to the overlap of the peaks, the increase of the chain fraction for increasing temperature is obvious. For **C4** at 6.5 mM the chain fraction increases from about 0.15 at 298 K to about 0.55 at 343 K. For **C6** at 8 mM the fraction of monomers in chains is lower than for **C4** as found earlier in the concentration-dependent experiments. The chain fraction also increases with temperature, from 0.14 at 298 K to about 0.40 at 343 K.

This temperature effect on the relative amounts of rings and chains yields a quite unusual temperature−viscosity dependence. Both compounds **C4** and **C6** (Zn^{2+}: ligand ratio = 1) show an increase in reduced viscosity upon heating due to ring opening (Figure 15). This effect is largest for **C4**. When the temperature is increased above 340 K, the viscosity decreases again slightly. For conventional covalent polymers, increasing the temperature results in a higher mobility of the chains and therefore in a decrease in viscosity. Also, for supramolecular polymers a decrease in viscosity is common upon heating,[25] although a hydrogen-bonded supramolecular polymer described by Folmer et al. shows a similar increase in viscosity upon heating due to ring opening.[26,27] The novelty of our system is that besides concentration and temperature also the metal−ligand ratio can be used to tune the system. To show the large effect of the metal−ligand ratio, also a curve is shown in Figure 15 for **C4** at a ratio of 1.02. The decrease in

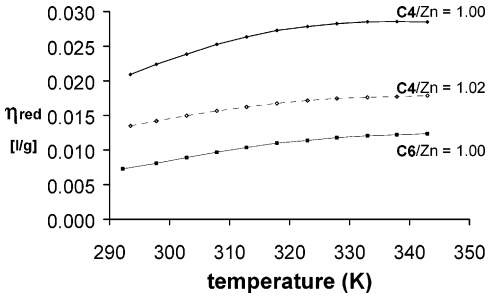

Figure 15. Reduced viscosity of ligands **C4** (37.8 mM) and **C6** (37.6 mM) as a function of temperature at a $Zn(ClO_4)_2$/ligand ratio close to 1 in 0.1 M PIPES buffer, pH 5.4.

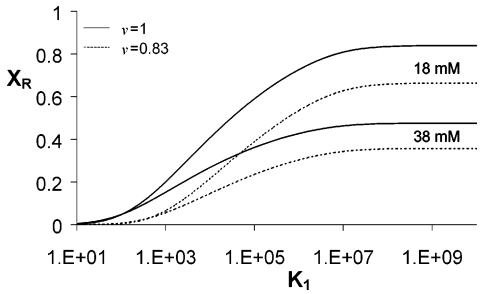

Figure 16. Theoretical: fraction of monomers in rings as a function of K_1 for $\nu = 0.83$ and $\nu = 1$ at two concentrations and $y = 1$. $K_2 = K_1/8$, $K_{a1} = K_1/50$, and $K_{a2} = K_1/2.5$.

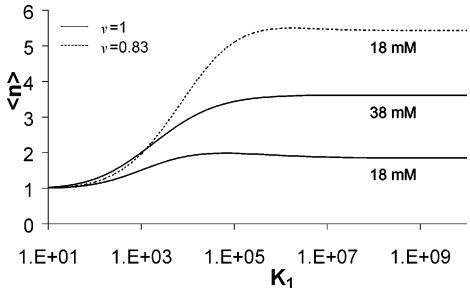

Figure 17. Theoretical: the average length as a function of K_1 for $\nu = 0.83$ and $\nu = 1$ at two concentrations and $y = 1$. $K_2 = K_1/8$, $K_{a1} = K_1/50$, and $K_{a2} = K_1/2.5$.

viscosity is very large for only a small change in ratio.

The effect of the temperature on the equilibrium between chains and rings, observed in the experiments, is a result of the variation of the stability constants K_1 and K_2 and the protonation constants K_{a1} and K_{a2} with temperature. With increasing temperature the stability constants become smaller. This results in a decrease of the fraction of monomers in rings, as shown in Figure 16 for both monomers, at two concentrations and for $y = 1$. The ratio between the different stability constants K_1, K_2, K_{a1}, and K_{a2} was fixed in these calculations. (Note that, in reality, the various stability constants may have a different temperature dependence, so that the ratio between them may vary with temperature.) The fraction of rings X_R increases with K and reaches a plateau at high K values. In this region the values of the stability constants are not very important for the ring−chain equilibrium. The effect of the stability constants on the average length is shown in Figure 17. It can be seen in this figure that for high values of the stability constants (low temperatures) the average length reaches a plateau. In this region, the calculations are not very sensitive to the K values. For small values of K_1, the average length decreases as K_1 decreases. At low monomer concentrations, the average length of the

chains may increase slightly and pass a maximum with decreasing K_1 (or increasing temperature). The reason for this is that some of the rings open up and form chains that are somewhat larger. At higher concentrations this effect cannot be observed. The slight increase in the average length may be the reason for the observed increase in viscosity with increasing temperature. For the concentrations used in Figure 15, however, such an increase could not be observed in the calculations. Nevertheless, the viscosity may still increase, even though the average length does not, because the contribution to the viscosity of a ring of certain length is probably smaller than that of a chain of the same length, because the structure of a ring is more compact. For a better interpretation of Figure 15, it is necessary to know how the stability constants are affected by the temperature. We have assumed in the calculations that the ratio between the different stability constants remains constant, which is not necessarily true.

We note furthermore that a decrease of the pH may have a similar effect as the temperature: the competition with protons also results in a decrease of the amount of rings and may therefore also result in an increase in viscosity.

In the derivation of the length distribution of rings, we have assumed that the polymers can be described as Gaussian chains, which is a reasonable assumption for long chains. However, since the average length reaches only a few Kuhn segments (see Figure 7), this assumption is certainly not valid. Therefore, we expect that the calculated data are not quantitatively correct for these small monomers, and we do not try to calculate viscosities from the theoretical data to make a more direct comparison. The qualitative agreement between the experiments and the calculations is very encouraging however. In principle, a more thorough comparison between the model and experiments should be possible for monomers with a longer spacer ($v \gg 1$), for which the Gaussian approximation is better.

V. Concluding Remarks

In conclusion, we presented here the first coordination polymers that are water-soluble at every metal:ligand ratio. The reversibility of the coordinative bonds is evident from the dependence of the viscosity and ^{1}H NMR measurements on the concentration ratio. For monomers with a spacer that is just long enough to form an intramolecular complex without strain, rings are dominant at low concentrations. This causes a minimum in the viscosity at a 1:1 metal:ligand ratio. The ring fraction at a 1:1 ratio of metal ions and ligands decreases with both increasing concentration and increasing temperature and it is lower for monomers with a shorter spacer. Reversible ring opening at higher temperatures causes an increase in viscosity, which is a rare phenomenon.

A model developed by Jacobson and Stockmayer was used to calculate the molecular weight distributions of chains and rings. The model is in qualitative agreement with the experimental results. In principle, a more direct comparison between theory and experiments would be possible for monomers with a longer spacer, for which the Gaussian chain assumption, adopted in the model, is better.

References and Notes

(1) Lehn, J.-M. *Supramolecular Chemistry, Concepts and Perspectives*; VCH: Weinheim, 1995.
(2) Ciferri, A. *Supramolecular Polymers*; Marcel Dekker: New York, 2000.
(3) Brunsveld, L.; Folmer, B. J. B.; Meijer, E. W.; Sijbesma, R. P. *Chem. Rev.* **2001**, *101*, 4071−4097.
(4) Zimmerman, N.; Moore, J. S.; Zimmerman, S. C. *Chem. Ind.* **1998**, 604−610.
(5) Whitesides, G. M.; Mathias, J. P.; Seto, C. T. *Science* **1991**, *254*, 1312−1319.
(6) Fogleman, E. A.; Yount, W. C.; Xu, J.; Craig, S. L. *Angew. Chem., Int. Ed.* **2002**, *41*, 4026−4028.
(7) Chen, H. C.; Cronin, J. A.; Archer, R. D. *Macromolecules* **1994**, *27*, 2174−2180.
(8) Kelch, S.; Rehahn, M. *Macromolecules* **1997**, *30*, 6185−6193.
(9) Bernhard, S.; Takada, K.; Déaz, D. J.; Abrũna, H. D.; Mürner, H. *J. Am. Chem. Soc.* **2001**, *123*, 10265−10271.
(10) Velten, U.; Rehahn, M. *Chem. Commun.* **1996**, 2639−2640.
(11) Velten, U.; Lahn, B.; Rehahn, M. *Macromol. Chem. Phys.* **1997**, *198*, 2789−2816.
(12) Lahn, B.; Rehahn, M. *e-Polym.* **2002**, *1*, 1−33.
(13) Schütte, M.; Kurth, D. G.; Linford, M. R.; Cölfen, H.; Möhwald, H. *Angew. Chem., Int. Ed.* **1998**, *37*, 2891−2893.
(14) Schubert, U. S.; Eschbaumer, C. *Angew. Chem., Int. Ed.* **2002**, *41*, 2892−2926.
(15) Schubert, U. S.; Eschbaumer, C. *Polym. Prepr.* **2000**, *41*, 676−677.
(16) Jacobson, H.; Stockmayer, W. H. *J. Chem. Phys.* **1950**, *18*, 1600−1606.
(17) Flory, P. J. *Chem. Rev.* **1946**, *39*, 137.
(18) Kuhn, W. *Kolloid Z.* **1934**, *68*, 2.
(19) Shimada, J.; Yamakawa, H. *Macromolecules* **1984**, *17*, 689−698.
(20) Cates, M. E.; Candau, S. J. *J. Phys.: Condens. Matter* **1990**, *2*, 6869.
(21) Chessa, G.; Scrivanti, A. *J. Chem, Soc., Perkin Trans 1* **1996**, 307−311.
(22) Liu, S.-G.; Liu, H.; Bandyopadhyay, K.; Gao, Z.; Echegoyen, L. *J. Org. Chem.* **2000**, *65*, 3292−3298.
(23) Anderegg, G. *Helv. Chim. Acta* **1960**, *43*, 414−424.
(24) Johnson, C. S., Jr. *Prog. Nucl. Magn. Spectrosc.* **1999**, *34*, 203−256.
(25) St. Poucain, C. B.; Griffin, A. C. *Macromolecules* **1995**, *28*, 4116−4121.
(26) Folmer, B. J. B.; Sijbesma, R. P.; Meijer, E. W. *J. Am. Chem. Soc.* **2001**, *123*, 2093−2094.
(27) Söntjens, S. H. M.; Sijbesma, R. P.; Van Genderen, M. H. P.; Meijer, E. W. *Macromolecules* **2001**, *34*, 3815−3818.

MA030353T